Targeted analysis of chondrocyte central metabolites in response to cyclical compression and shear deformations

[1]Erik P. Myers, [1]Aurora Gallagher, [1]Avery Welfley, [1]Samuel Battles, [1]Aidan Gregory, [1]Priyanka Brahmachary, [2]Mark Greenwood, and [1,3]Ronald K. June

Affiliations

[1]Department of Mechanical & Industrial Engineering, Montana State University, Bozeman MT.

[2]Department of Mathematical Sciences, Montana State University, Bozeman MT.

[3]Department of Microbiology & Cell Biology, Montana State University, Bozeman MT.

*Corresponding Author:

Ronald K. June, Ph.D.

Department of Mechanical & Industrial Engineering, Montana State University

PO Box 173800, Bozeman, MT 59717-3800 | Phone: (406) 994-5941; Fax: (406) 994-6292; E-mail: rjune@montana.edu

Abstract

Osteoarthritis results in deterioration of articular cartilage, the soft tissue covering articulating surfaces of bones in joints like the knee and hip. Cyclical mechanical stimulation of articular cartilage results in synthesis of cartilage matrix, suggesting that therapeutic mechanical stimulation might be beneficial for cartilage repair in osteoarthritis. Several prior studies identify ion channels and cytoskeletal molecules as components of chondrocyte mechanotransduction. The pathways of central metabolism, glycolysis, the pentose phosphate pathway, and the tricarboxylic acid cycle are necessary for producing non-essential amino acids that are needed for synthesizing matrix proteins for cartilage repair. However, it is currently unknown if and how levels of central metabolites change with applied mechanical stimulation of chondrocytes. Here, we show that applied cyclical shear and compressive deformations drive changes in multiple central metabolites in primary chondrocytes. These results add to a rich picture of chondrocyte mechanotransduction, including calcium signaling, ion channels, integrins, and cytoskeletal components. By finding compression- and shear-induced changes in central metabolites, these data support the potential for therapeutic mechanotransduction toward cartilage repair. Future studies may build on these results to understand the relationships between mechanical stimulation and chondrocyte central metabolism.

Keywords

cartilage; chondrocyte; mechanotransduction; osteoarthritis; metabolism

Introduction

Articular cartilage is the soft tissue lining diarthrodial joints like the knee and hip. This tissue contains a single cell type—the articular chondrocyte—and is subjected to cyclical loads during daily activities such as walking.These loads cause tissue-level deformations that result in mechanical stimulation of chondrocytes. Tissue-level deformations include tension, compression, and shear-based on *in vivo* measurements (Chan et al. 2016).

A key feature of the most common joint disease, osteoarthritis (OA), is the deterioration of articular cartilage (Tonge et al. 2014).This deterioration results in alterations of both the extracellular and pericellular cartilage matrices, with concomitant changes in various cartilage mechanical properties. For example, after joint injury, there are significant decreases in the indentation modulus of the mouse pericellular matrix after just 3 days, with a reduction of ~50% after 1 month (Chery et al. 2020). In contrast, exercise typically results in improved cartilage health. Patients with a history of marathon running had ~25% thicker cartilage than age-matched controls (Mosher et al. 2010).

Early observations show that cyclical mechanical stimulation of cartilage and chondrocytes results in production of matrix molecules (Mauck et al. 2006; Sah et al. 1989) through chondrocyte mechanotransduction. This shows that mechanical stimulation can drive therapeutic production of matrix for cartilage repair. While several ion channels (Ely et al. 2025) and various cytoskeletal components (Haudenschild et al. 2011; Ohashi et al. 2006) have been implicated in chondrocyte mechanotransduction, many questions remain regarding the specific cascade of signals that results in increased matrix production.

67 Central metabolism (*i.e.* energy metabolism) is a network of enzymes and small-
68 molecule intermediates called metabolites used by cells to harvest carbon and energy to
69 support cellular function. Substrates include glucose and glutamine, which can be
70 metabolized to produce non-essential amino acids. Functioning central metabolism,
71 including both glycolysis and cellular respiration, involves oxygen consumption and is
72 essential for producing the non-essential amino acids required for cartilage regeneration.
73 For example, non-essential amino acids make up 83.1, 71.4, and 74.5% of the primary
74 sequences for the key cartilage matrix proteins encoded by COL2A1, COL6A1, and
75 ACAN (types II and VI collagen and aggrecan).

76 We hypothesized that mechanical stimulation would alter the production of central
77 metabolites in articular chondrocytes. Toward this goal, we harvested articular
78 chondrocytes, expanded them in monolayer culture, and then encapsulated them in
79 physiologically stiff agarose (Jutila et al. 2015; Zignego et al. 2014). Embedded
80 chondrocytes were then stimulated with cyclical shear and compressive strains at
81 physiological levels. Immediately after mechanical stimulation, metabolites were
82 extracted. Quantification of central metabolites was performed using targeted
83 metabolomic profiling. We found changes in levels of several metabolites, demonstrating
84 that mechanical stimulation affects chondrocyte central metabolism. These results can
85 inform future studies on how mechanical stimuli influence chondrocyte metabolism for
86 cartilage maintenance and repair strategies.

87 **Methods**

88 Chondrocyte Harvest and Culture

89 To assess central metabolism in chondrocyte mechanotransduction, chondrocytes
90 were isolated from cartilage using established methods (Zignego et al. 2015; Zignego et
91 al. 2014). Primary Human Chondrocytes (PHCs) were obtained from discarded tissue
92 from Stage-IV osteoarthritis patients (n=5 male and n=5 female) undergoing total joint
93 replacement under IRB approval. Bovine chondrocytes (BCs, n=5) were harvested from
94 knee joints of 18–22-month-old cattle obtained from a local abattoir. Articular cartilage
95 was digested with Type I Collagenase (2 mg/mL in DMEM with penicillin and
96 streptomycin, Gibco, Waltham, MA, USA) for 14 h at 37 ºC. Isolated chondrocytes were
97 cultured in Dulbecco's Modified Eagle's medium (DMEM, Gibco, Waltham, MA, USA)
98 supplemented with Fetal Bovine Serum (FBS, 10% v/v, Bio-Techne, Minneapolis, MN,
99 USA), penicillin (10,000 I.U./mL), and streptomycin (10,000 µg/mL, Sigma, St. Louis, MO,
100 USA) in 5% CO2 at 37 ºC. First passage cells were used for experiments.

101 To provide a three-dimensional environment in the range of physiological stiffness,
102 chondrocytes were encapsulated in high-stiffness agarose (Jutila et al. 2015). After
103 trypsinization, cells were washed with 1X PBS and resuspended in DMEM (without
104 phenol red) and mixed with low-melting-temperature agarose (Type VII-A

105 Sigma Aldrich) at a final concentration of 4.5% wt/vol with ~500,000 cells/gel and
106 allowed to solidify for 10 min. Hydrogels were cast in a cylindrical aluminum mold to have
107 a nominal diameter of 0.5" and a height of 0.25" following a previously established
108 protocol (Jutila et al. 2015), which results in chondrocyte viability >90% (Zignego et al.

109 2014). Agarose gels were placed in 24-well tissue culture plates (Falcon) with 2 mL
110 custom DMEM media containing 4.5g/L glucose, 2 mM L-glutamine,110mg/L sodium
111 pyruvate, 10% FBS, and 1% PenStrep and cultured overnight in 5% CO_2 at 37ºC. Prior
112 to loading, media was replaced with PBS for 1 hr and incubated in 5% CO_2 at 37ºC.

113

114 Mechanical Stimulation

115 To evaluate the effects of physiological loading on chondrocyte central metabolism,
116 agarose-embedded chondrocytes were subjected to different mechanical stimuli. Stimuli
117 included applied cyclical shear and compressive strains in a tissue culture environment
118 (Figure 1, Supplemental Material 1). A total of N=10 PHCs (n=5 male and n=5 female)
119 and N=5 BC samples were used.

120 Chondrocyte-embedded agarose constructs from each bovine or human donor were
121 randomized into five experimental groups: unloaded controls (U), 15 minutes of cyclical
122 compressive strain (15C), 15 minutes of cyclical shear strain (15S), 30 minutes of cyclical
123 compressive strain (30C), and 30 minutes of cyclical shear strain (30S). For both
124 compressive and shear stimulation, mean strains were 5% with an amplitude of 2.5%.
125 Each experiment was performed at 1.1Hz with 5% preload applied initially for 15 minutes
126 to allow for stress relaxation. Mechanical stimulation of samples from each donor was
127 completed over the course of a single day. In instances where multiple donors were
128 available on the same day, simultaneous loading for each group across all available
129 donors was performed.

For each loading group, the hydrogel was removed from PBS, placed within the polysulfone sample cup, and resubmerged in fresh PBS to prevent drying during loading (Figure 1). The bioreactor was then placed inside the Tri-GAS incubator and powered on to provide mechanical stimulation within a tissue culture environment. In the case of an uneven number of hydrogels, a cell-free agarose sample was used to balance the load from the hydrogels on the plunger plate.

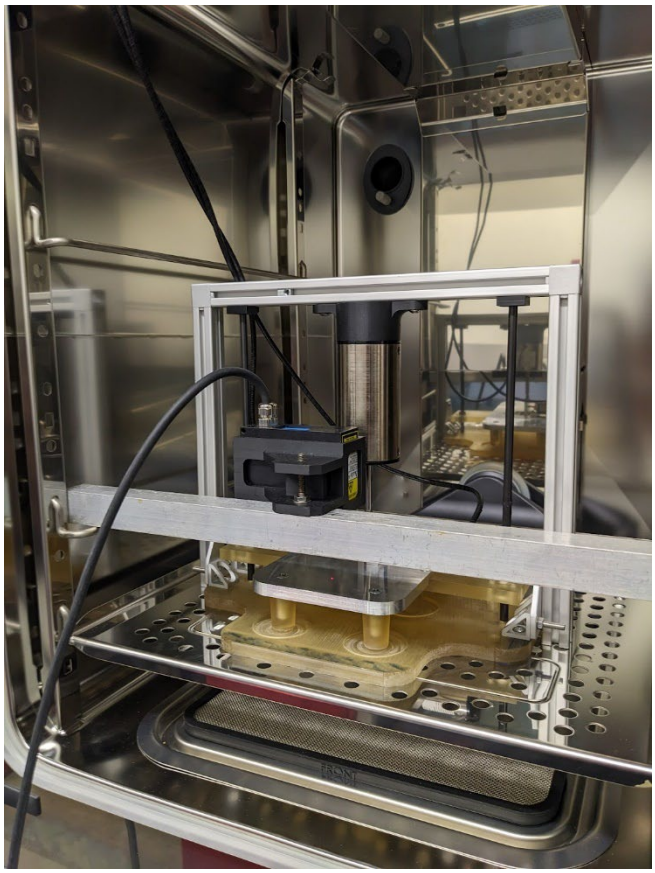

Figure 1: Chondrocyte bioreactor inside a Tri-Gas incubator with laser displacement sensor suspended overhead. During normal experimentation, the sensor is absent from the incubator.

Immediately after mechanical stimulation, hydrogels were removed from the bioreactor and bisected using a sterile scalpel. One-half of the sample was used for oxygen measurement and the other half was used for targeted metabolomic analysis.

Oxygen Measurement and Metabolite Extraction

An oxygen measurement system (OX-10, Unisense, Aarhus, Denmark) was used to quantify oxygen tension immediately after mechanical stimulation. Probes were calibrated to 0% O_2 tension using a nitrogen sparged water bath and 100% O_2 tension using an atmospheric air sparged water bath. 2-point calibration curves were then used to quantify oxygen saturation readings from each sample bisect. The oxygen probe was inserted into the hydrogel and oxygen readings were measured for 1 minute, with the minimum oxygen tension during the measurement recorded for each sample (Figure 2).

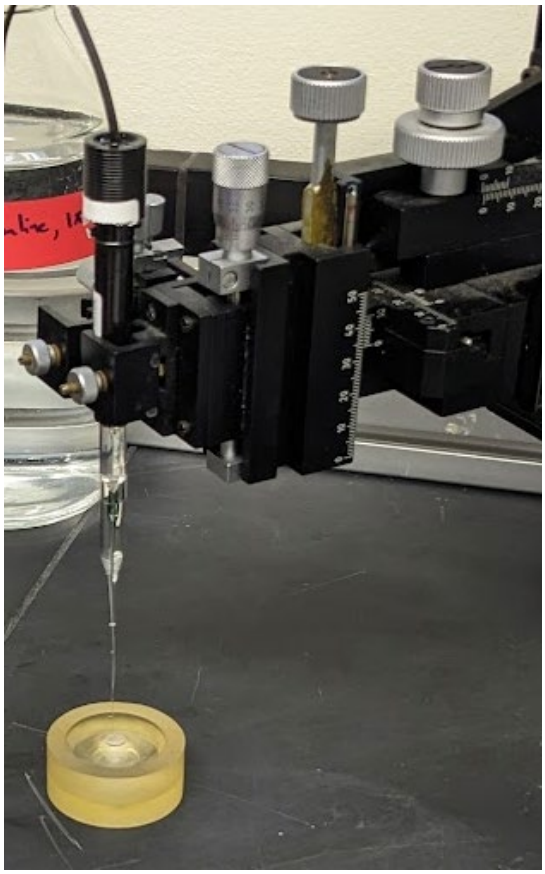

Figure 2: Oxygen probe needle embedded within an agarose hydrogel. The probe was retracted after each reading and used to collect a pre and post reading atmospheric baseline.

155 The remaining half of the hydrogel was immediately wrapped in autoclaved aluminum
156 foil and flash-frozen in liquid nitrogen to preserve metabolite levels after mechanical
157 stimulation. After freezing for 1-2 minutes, the gel was crushed using a sterile aluminum
158 rod. The pulverized hydrogel was then placed in a 2.5mL Eppendorf tube and allowed to
159 freeze in -80°C overnight. This process was completed for all hydrogels for all
160 experimental groups. After freezing for at least 12 hours, the crushed gels were removed
161 from the freezer and homogenized into a powder using a Cryomill (Verder Scientific,
162 Haan, Germany).

163 Following homogenization, the powder was suspended in extraction buffer (70:30:1%
164 Methanol:Acetone:Formic acid). Formic acid facilitated metabolite release from the
165 homogenized agarose (Supplemental Material 2). Each hydrogel bisect was extracted
166 with 5mL of extraction buffer at -80°C overnight. The following morning, samples were
167 centrifuged (4,000 rpm, 10 minutes), and the supernatant was evaporated using a
168 vacuum centrifuge at 45°C (Eppendorf, Hamburg, Germany) until only the dried pellet of
169 concentrated metabolites remained. These metabolite pellets were then resuspended in
170 50μL 50:50 HPLC water:acetonitrile and sent for mass spectrometry analysis.

171 Mass spectrometry analysis of mechanically stimulated constructs

172 After metabolite extraction, levels of central metabolites were quantified using liquid
173 chromatography-mass spectrometry (LC-MS) using an established protocol
174 (Brahmachary et al. 2023) optimized for an Agilent 6538 Q-TOF (C18 Column). Quality
175 control included analysis of blank samples of 50:50 HPLC Water:Acetonitrile every ten
176 samples. For quantification, analytical standards containing 18 key central carbon
177 metabolites were included within the run at concentrations of 1-100 μg/mL. Individual

178 calibration curves were constructed based on the known standard concentration and the
179 measured metabolite intensity (Supplemental Material 3). A pool was created for each
180 loading group and assembled from 5 randomly chosen 10μL samples from each group to
181 aid in fragmentation and identification of each standard metabolite in the sample. After
182 LC-MS analysis, data were converted to concentrations from intensities using the
183 calibration curves before statistical analysis and visualization.

184 Statistical Analysis of Metabolites

185 After removing outliers due to metabolite extraction challenges (Supplemental
186 Material 2), the data from the remaining n=3 male human, n=3 female human, and n=5
187 bovine donors were combined for a total of 65 samples and analyzed on a per-metabolite
188 basis. Eighteen standard metabolites were used for mass spectrometry calibration; two
189 different forms of NADH as well as HSCoA and oxaloacetate were not detected
190 consistently in the experimental samples, leaving a total of 14 central metabolites for
191 comparison (Supplemental Material 2-3). Metabolites, their pathways within central
192 carbon metabolism, and the significance of mean differences with the unloaded controls
193 were recorded for all 14 detected metabolites (Table 1).

194 *Table 1: Individual metabolites, their pathways, and statistical results. ANOVA p-*
195 *value is the p-value for the repeated measures ANOVA. Significant groups indicate*
196 *groups significantly different from unloaded controls with arrows indicating increased (↑)*
197 *or decreased (↓) levels.*

198

Metabolite	Pathway	ANOVA p-value	Significant Groups vs Unloaded Ctrl
Fructose / Glucose (Glucose)	Glycolysis	0.035	↓30C, ↓30S
Fructose-6-phosphate	Glycolysis	0.488	

Phosphoenolpyruvic Acid (PEP)	Glycolysis	0.641	
Pyruvic Acid (Pyruvate)	Glycolysis	0.0046	↓30C
Lactic Acid (Lactate)	Glycolysis	0.220	
6-p-gluconate	PPP	0.747	
Sedoheptulose-7-phosphate	PPP	0.187	
Citric Acid (Citrate)	TCA Cycle	0.615	
2-Oxoglutaric Acid (α-ketoglutarate)	TCA Cycle	0.0984	
Succinic Acid (Succinate)	TCA Cycle	0.125	↑30S
Fumaric Acid (Fumarate)	TCA Cycle	0.358	
Malic Acid (Malate)	TCA Cycle	0.0005	↓30C, ↓30S
Glutamic Acid (Glutamine)	TCA Cycle	0.211	
Glutamine	TCA Cycle	0.0085	↓15C, ↓30C, ↓15S, ↓30S

For each of the detectable 14 metabolites, statistical analysis was performed using Graphpad Prism. Outlier identification was performed using the method of Motulsky and Brown (ROUT in Prism) with a false discovery rate of 1% (Motulsky and Brown 2006). One-way repeated measures ANOVA was performed on log-transformed data to test for differences in mean concentrations between the experimental groups. To control the family-wise error rate, additional pairwise comparisons were performed using Tukey's HSD. T-tests were used to compare metabolite levels between chondrocytes from male and female donors using the Holm-Sidak correction for multiple testing between experimental groups without assuming sphericity. Metabolites with significant differences are visualized using violin plots. All metabolite data is available in Supplemental Material 4.

Results

Oxygen Concentration

Because oxygen is consumed during cellular respiration, oxygen readings were sampled for each hydrogel during experimentation. Statistical analysis of the oxygen

216 readings revealed no significant differences in oxygen tension regardless of loading
217 condition. This may indicate that there was not sufficient time for chondrocytes to utilize
218 measurable oxygen during the short time span (0-30 minutes) of the mechanical
219 stimulation. Oxygen data are available in Supplemental Material 5.

220 Targeted Metabolomics

221 Toward understanding how mechanical stimuli affect chondrocyte central metabolite
222 levels, we performed targeted metabolomic profiling after cyclical shear and compressive
223 stimulation. Five of the fourteen measured metabolites resulted in at least one significant
224 between-group difference. Of these five, two are related to glycolysis (Figure 3) and three
225 are related to the TCA cycle (Figure 4). Four metabolites decreased in quantity in the
226 mechanically stimulated groups, suggesting that mechanical stimulation either decreased
227 production or increased consumption of these metabolites. For the human OA donors,
228 there were no detected differences in any measured metabolite levels between male and
229 female donors (minimum n=3 each). Oxaloacetate, NADH1, HSCoA, and NADH2 were
230 not consistently detected amongst the samples and were not analyzed further, and there
231 were no differences in pentose phosphate metabolites (Figure 5.).

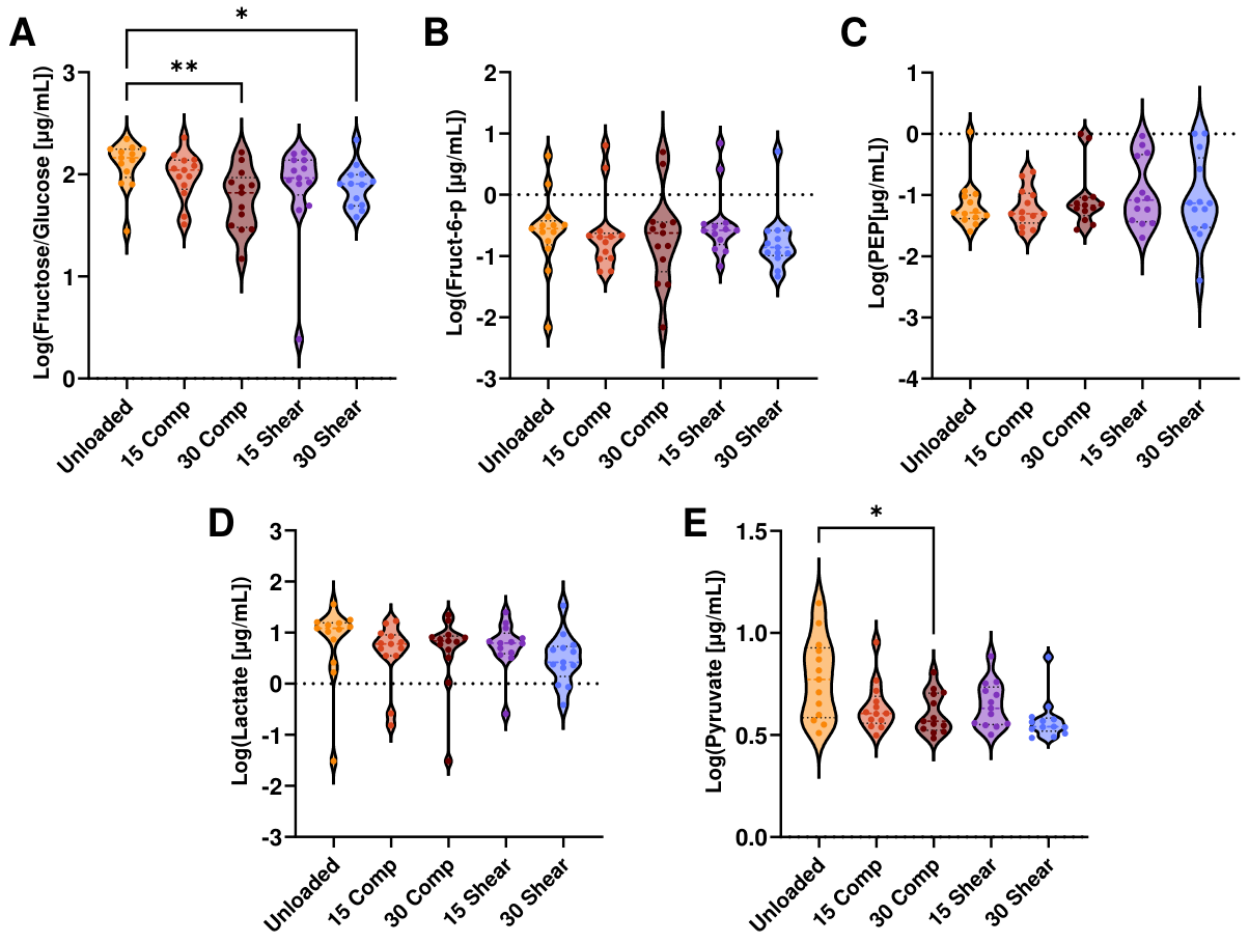

*Figure 3: Concentrations of glycolytic metabolites in response to shear and compressive mechanical stimulation. (A) Fructose/Glucose. (B) Fructose-6-phosphage. (C) Phosphoenolpyruvate. (D) Lactate. (E) Pyruvate. * indicates p<0.05 and ** indicates p<0.01 upon Holm-Sidak post hoc test between experimental groups. n=11 per group.*

Glucose, the input to glycolysis, decreased after both 30 minutes of cyclical compression and shear compared to unloaded controls (Figure 3A). Glucose concentrations were substantially higher than other metabolites because of the initial culture in media with 4.5g/L glucose. Pyruvate, an end product of glycolysis, decreased in response to 30 minutes of shear and compression stimulation (Figure 3E). In anaerobic respiration, pyruvate can be converted to lactate, but there were no significant differences in mean lactate after mechanical stimulation. These results indicate that there was substantial

245 consumption of glycolytic metabolites in response to both applied shear and compression
246 for chondrocytes.

247 Within the TCA cycle, succinate increased after 30 minutes of shear stimulation
248 compared to controls (Figure 4C). Malate levels decreased after 30 minutes of both
249 compression and shear stimulation (Figure 4E). Glutamine, a carbon source for the TCA
250 cycle, levels decreased for both 15 and 30 minutes of compression and shear compared
251 to unloaded controls (Figure 4G). These data indicate that cyclical shear and
252 compression induced substantial TCA activity in articular chondrocytes.

253

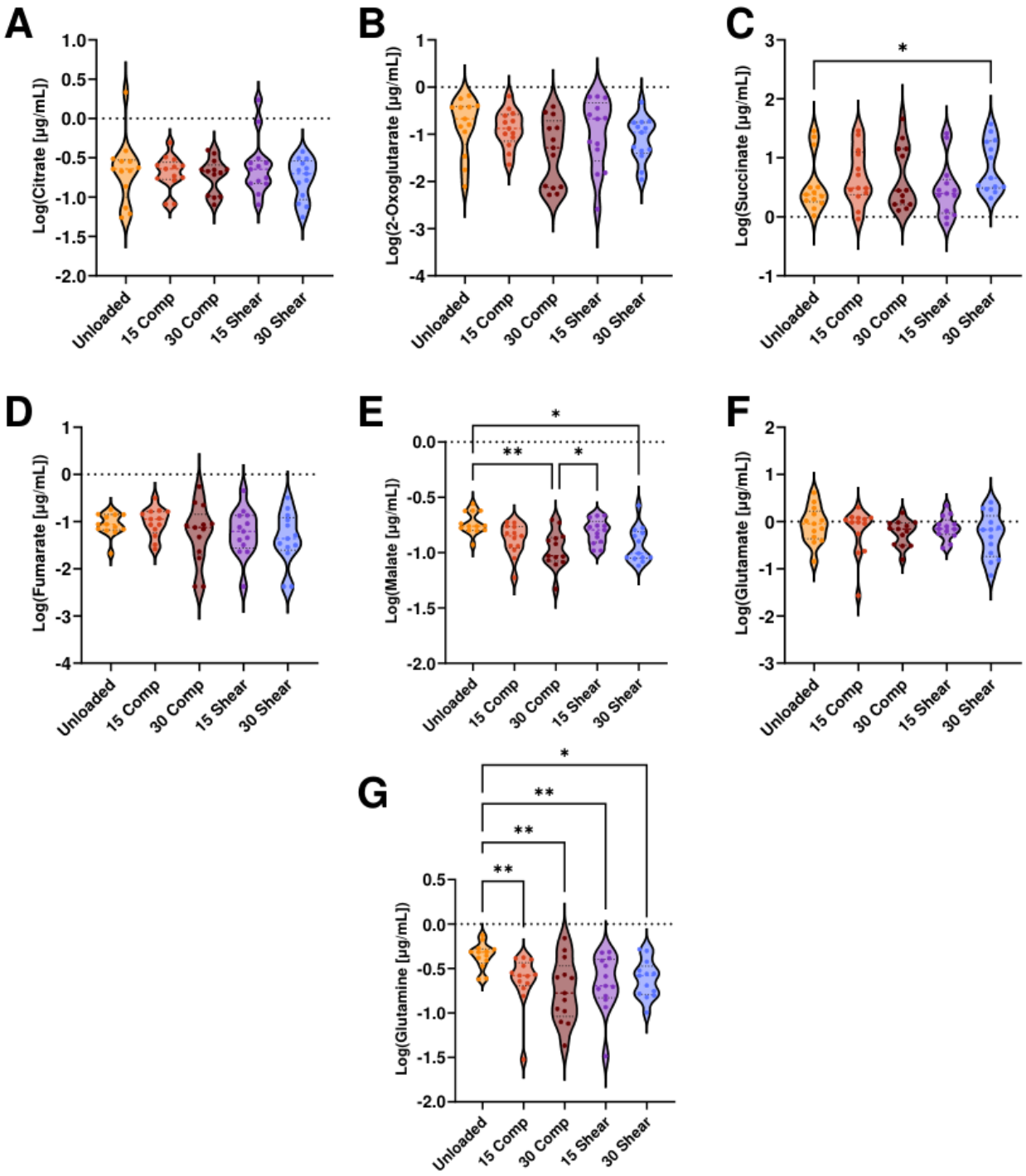

*Figure 4: Concentrations of TCA metabolites in response to shear and compressive mechanical stimulation. (A) Citrate. (B) 2-Oxoglytarate. (C) Succinate. (D) Fumarate. (E) Malate. (F) Glutamate. (G) Glutamine. * indicates $p<0.05$ and ** indicates $p<0.01$ upon Holm-Sidak post hoc test between experimental groups. n=11 per group.*

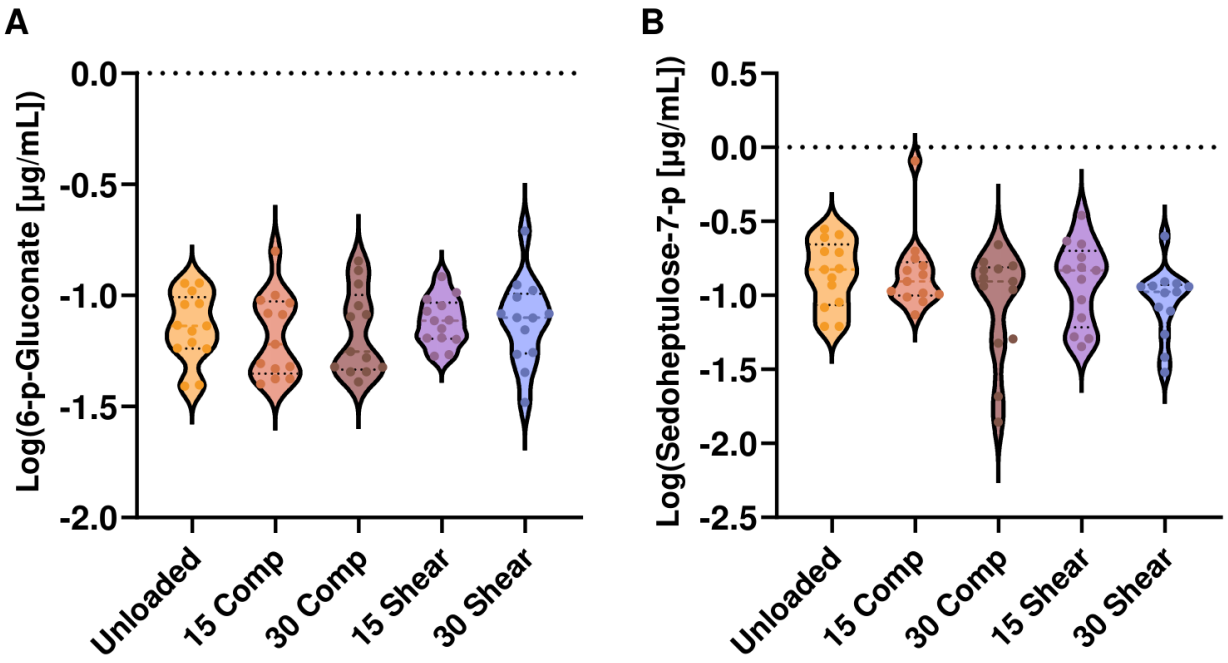

Figure 5: Concentrations of Pentose Phosphate Pathway metabolites in response to shear and compressive mechanical stimulation. (A) 6-phospho-gluconate. (B) sedoheptulose-7-phosphate. No significant differences observed. n=11 per group.

Discussion

This study examined the role of cyclical mechanical stimulation in chondrocyte metabolism using targeted profiling of metabolites from glycolysis, the pentose-phosphate pathway, and the TCA cycle. Mechanical loading altered several key metabolites, revealing that chondrocyte metabolism dynamically responds to cyclical shear and compressive stimuli. However, given the complexity of these larger biochemical networks, changes in metabolite abundance may reflect altered production and/or consumption (Doran et al. 2024).

274 Glycolytic metabolites (glucose and pyruvate) were decreased in mechanically
275 stimulated samples compared to unloaded controls, suggesting decreased production or
276 increased consumption, or a combination thereof. This may indicate a shift toward a
277 glycolytic, Warburg-like profile often seen in pathological conditions (Jiang et al. 2023) or
278 increased fueling of the TCA cycle to promote production of non-essential amino acids for
279 production of matrix proteins. Glutamine—a primary carbon source for the TCA cycle—
280 was similarly reduced in all mechanically stimulated groups compared to unloaded
281 controls, demonstrating changes in glutamine metabolism because of mechanical
282 stimulation. This reduction in glutamine following mechanical loading suggests enhanced
283 glutaminolysis, where glutamine is converted to glutamate and subsequently to α-
284 ketoglutarate to support increased TCA cycle activity. In parallel, it is possible that
285 glutamate can also be diverted toward proline biosynthesis to support matrix remodeling,
286 together explaining the observed drop in glutamine levels.

287 Conversely, succinate levels increased after 30 minutes of shear stimulation,
288 which may be linked to downstream redox signaling or mitochondrial stress, as
289 supported by findings in osteoarthritic bone tissues (Shodiev et al. 2024). Collectively,
290 this altered TCA activity suggests that mechanical loading increases energy demand
291 and may shift chondrocyte metabolism toward pathways that support the production of
292 non-essential amino acids for protein and matrix production.

293 Beyond this system, our findings may have broader implications for cyclical
294 loading in osteoarthritis progression. The effect of mechanotransduction on central
295 metabolism and signaling is increasingly recognized in all joint tissues (Zhao et al.
296 2020). These results support the emerging evidence that metabolism is not a passive

297 outcome of chondrocyte function, but rather a key response to mechanical signals. In
298 healthy tissue, enhanced mitochondrial metabolism under physiological loading
299 supports ECM synthesis and redox homeostasis (Coleman et al. 2016). In contrast,
300 excessive loading can promote glycolytic upregulation and impaired mitochondrial
301 respiration, leading to an accumulation of metabolic intermediates and reactive oxygen
302 species that activate inflammatory signaling cascades and cytokine expression (Huang
303 et al. 2023; Tan et al. 2022). Thus, these mechanically induced metabolomic changes
304 may serve as both a mechanism of adaptation and a contributor to degeneration,
305 depending on the cellular context and load magnitude, underscoring their potential as
306 therapeutic modulators of cartilage metabolism.

307 A key limitation of this study is that these targeted metabolomic profiles only
308 provide a static snapshot of metabolite levels at 15-minute time intervals, limiting the
309 interpretability of metabolic flux. Additionally, measuring oxygen consumption
310 immediately after loading may not provide sufficient time for chondrocytes to
311 appreciably consume oxygen within the agarose, and later timepoints may provide
312 additional insights. Future studies should utilize stoichiometric modeling to better
313 understand how mechanical stimulation influences flux of central metabolites and might
314 also incorporate improved temporal resolution with metabolite biosensors in live cell
315 imaging, functional assays, and isotope tracing to better resolve metabolic flux and
316 pathway dynamics. These methods would help quantify nutrient utilization and identify
317 specific biochemical reactions altered by mechanical stimuli. Given the small sample
318 size (n=3 each) of male and female donors, future studies should further explore
319 potential sex differences, hormonal influences, and mitochondrial regulation. These

findings could ultimately guide regenerative medicine approaches for OA by identifying optimal mechanical loading parameters that support metabolism-based repair and maintenance of articular cartilage.

Acknowledgements

This study was funded by research grants from the NIH (NIAMS R01AR073964 and R01AR081489) and NSF (CMMI 1554708).

Supplemental Material

1. Bioreactor Design
2. Metabolite Extraction and Outlier Analysis (formerly Supp Mat B)
3. Metabolite Calibration Curves (formerly Supp Mat C)
4. Raw Metabolite Data
5. Raw Oxygen Data

References

Brahmachary PP, Welhaven HD, June RK (2023) Metabolomic Profiling to Understand Chondrocyte Metabolism Methods Mol Biol 2598:141-156 doi:10.1007/978-1-0716-2839-3_11

Chan DD, Cai L, Butz KD, Trippel SB, Nauman EA, Neu CP (2016) In vivo articular cartilage deformation: noninvasive quantification of intratissue strain during joint contact in the human knee Sci Rep 6:19220 doi:10.1038/srep19220

Chery DR et al. (2020) Early changes in cartilage pericellular matrix micromechanobiology portend the onset of post-traumatic osteoarthritis Acta Biomater 111:267-278 doi:10.1016/j.actbio.2020.05.005

Coleman MC, Ramakrishnan PS, Brouillette MJ, Martin JA (2016) Injurious Loading of Articular Cartilage Compromises Chondrocyte Respiratory Function Arthritis Rheumatol 68:662-671 doi:10.1002/art.39460

Doran PM, Morrissey K, Carlson RP (2024) Bioprocess Engineering Principles. 3rd Edition edn. Academic Press,

348 Ely EV et al. (2025) Chondrocyte-specific knockout of Piezo1 and Piezo2 protects against
349 post-traumatic osteoarthritis structural damage and pain in mice Arthritis Res Ther
350 27:152 doi:10.1186/s13075-025-03620-w

351 Haudenschild DR, Chen J, Pang N, Steklov N, Grogan SP, Lotz MK, D'Lima DD (2011)
352 Vimentin contributes to changes in chondrocyte stiffness in osteoarthritis J Orthop
353 Res 29:20-25 doi:10.1002/jor.21198

354 Huang YF et al. (2023) Lactate-upregulated NADPH-dependent NOX4 expression via
355 HCAR1/PI3K pathway contributes to ROS-induced osteoarthritis chondrocyte
356 damage Redox Biol 67:102867 doi:10.1016/j.redox.2023.102867

357 Jiang D, Guo J, Liu Y, Li W, Lu D (2023) Glycolysis: an emerging regulator of osteoarthritis
358 Front Immunol 14:1327852 doi:10.3389/fimmu.2023.1327852

359 Jutila AA, Zignego DL, Schell WJ, June RK (2015) Encapsulation of chondrocytes in high-
360 stiffness agarose microenvironments for in vitro modeling of osteoarthritis
361 mechanotransduction Ann Biomed Eng 43:1132-1144 doi:10.1007/s10439-014-
362 1183-5

363 Mauck RL, Yuan X, Tuan RS (2006) Chondrogenic differentiation and functional
364 maturation of bovine mesenchymal stem cells in long-term agarose culture
365 Osteoarthritis Cartilage 14:179-189 doi:10.1016/j.joca.2005.09.002

366 Mosher TJ, Liu Y, Torok CM (2010) Functional cartilage MRI T2 mapping: evaluating the
367 effect of age and training on knee cartilage response to running Osteoarthritis
368 Cartilage 18:358-364 doi:10.1016/j.joca.2009.11.011

369 Motulsky HJ, Brown RE (2006) Detecting outliers when fitting data with nonlinear
370 regression - a new method based on robust nonlinear regression and the false
371 discovery rate BMC Bioinformatics 7:123 doi:10.1186/1471-2105-7-123

372 Ohashi T, Hagiwara M, Bader DL, Knight MM (2006) Intracellular mechanics and
373 mechanotransduction associated with chondrocyte deformation during pipette
374 aspiration Biorheology 43:201-214

375 Sah RL, Kim YJ, Doong JY, Grodzinsky AJ, Plaas AH, Sandy JD (1989) Biosynthetic
376 response of cartilage explants to dynamic compression J Orthop Res 7:619-636
377 doi:10.1002/jor.1100070502

378 Shodiev DR, Zvyagina VI, Ryabova MN, Marsyanova YA (2024) Succinate-receptor
379 system of bone and cartilage tissue in patients with metabolic phenotype of
380 osteoarthritis BMP-chemistry 27:41-49 doi:10.29296/25877313-2024-09-06

381 Tan C, Li L, Han J, Xu K, Liu X (2022) A new strategy for osteoarthritis therapy: Inhibition
382 of glycolysis Front Pharmacol 13:1057229 doi:10.3389/fphar.2022.1057229

383 Tonge DP, Pearson MJ, Jones SW (2014) The hallmarks of osteoarthritis and the potential
384 to develop personalised disease-modifying pharmacological therapeutics
385 Osteoarthritis Cartilage 22:609-621 doi:10.1016/j.joca.2014.03.004

386 Zhao Z, Li Y, Wang M, Zhao S, Zhao Z, Fang J (2020) Mechanotransduction pathways in
387 the regulation of cartilage chondrocyte homoeostasis J Cell Mol Med 24:5408-
388 5419 doi:10.1111/jcmm.15204

389 Zignego DL, Hilmer JK, June RK (2015) Mechanotransduction in primary human
390 osteoarthritic chondrocytes is mediated by metabolism of energy, lipids, and amino
391 acids J Biomech 48:4253-4261 doi:10.1016/j.jbiomech.2015.10.038

392 Zignego DL, Jutila AA, Gelbke MK, Gannon DM, June RK (2014) The mechanical
393 microenvironment of high concentration agarose for applying deformation to
394 primary chondrocytes J Biomech 47:2143-2148
395 doi:10.1016/j.jbiomech.2013.10.051

396